IOP Publishing Nanotechnology
Nanotechnology **25** (2014) 312001 (15pp) doi:10.1088/0957-4484/25/31/312001

Topical Review

Reassembly of S-layer proteins

Dietmar Pum and Uwe B Sleytr

Institute of Biophysics, Department of Nanobiotechnology, University of Natural Resources and Life Sciences, Vienna, Muthgasse 11, 1190 Vienna, Austria

E-mail: dietmar.pum@boku.ac.at

Received 25 September 2013, revised 14 March 2014
Accepted for publication 31 March 2014
Published 17 July 2014

Abstract

Crystalline bacterial cell surface layers (S-layers) represent the outermost cell envelope component in a broad range of bacteria and archaea. They are monomolecular arrays composed of a single protein or glycoprotein species and represent the simplest biological membranes developed during evolution. They are highly porous protein mesh works with unit cell sizes in the range of 3 to 30 nm, and pore sizes of 2 to 8 nm. S-layers are usually 5 to 20 nm thick (in archaea, up to 70 nm). S-layer proteins are one of the most abundant biopolymers on earth. One of their key features, and the focus of this review, is the intrinsic capability of isolated native and recombinant S-layer proteins to form self-assembled mono- or double layers in suspension, at solid supports, the air-water interface, planar lipid films, liposomes, nanocapsules, and nanoparticles. The reassembly is entropy-driven and a fascinating example of matrix assembly following a multistage, non-classical pathway in which the process of S-layer protein folding is directly linked with assembly into extended clusters. Moreover, basic research on the structure, synthesis, genetics, assembly, and function of S-layer proteins laid the foundation for their application in novel approaches in biotechnology, biomimetics, synthetic biology, and nanotechnology.

Keywords: crystalline cell surface layers (S-layers), non-classical assembly pathway, matrix assembly, biomimetics, synthetic biology, bionanotechnology

(Some figures may appear in colour only in the online journal)

1. Introduction

A broad range of self-assembly systems has been developed by nature during billions of years of evolution. Most often their bottom-up-based construction principles are well understood and the molecular building blocks fully characterized. Among the well-established self-assembly systems, such as DNA lattices and polyhedra [14, 82, 98, 136], or self-assembled monolayers (SAMs) [125, 134], is the further exampleof crystalline archaeal and bacterial cell surface layers, termed *S-layers* [1, 5, 29, 103, 109, 115].

S-layers cover the cells completely and fulfill various functions [1, 29, 115]. Examples are their molecular sieving properties [89, 118] or their shape determination as a rigid corset for various archaeal cells [1, 26, 61, 72, 135]. But one of the most remarkable properties of isolated S-layer proteins is their capability to form free-floating self-assembly products in bulk solution (e.g. flat sheets, tubes, vesicles), to reassemble into extended mono- and double layers at solid supports, at the air-water interface, at lipid films, and to cover liposomes, nanocapsules, and nanoparticles completely [77, 107, 109, 114]. Moreover, most recently it was found that the dynamics in the formation of S-layer lattices follows a non-classical, multistage crystallization pathway [15, 17, 101, 120, 137]. However, S-layers are also fascinating patterning elements in bionanotechnology for increasing the robustness of biomimetic lipid membranes or for functionalizing various technologically relevant surfaces [24, 93, 95, 115].

This review gives an overview on the recrystallization of native and genetically modified S-layer proteins in solution

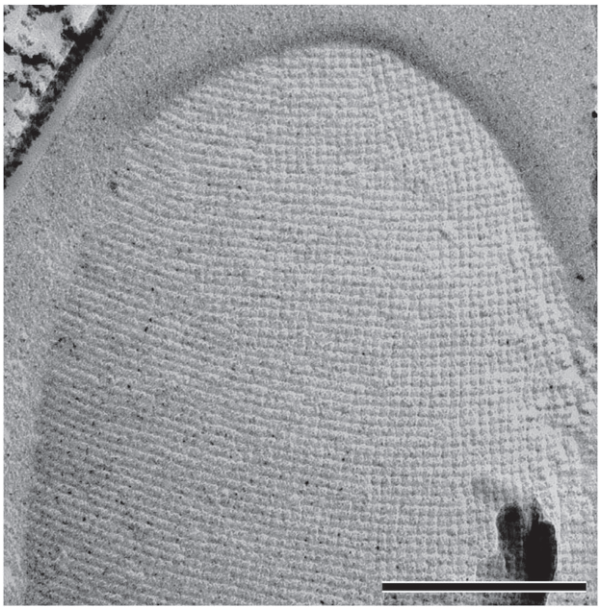

Figure1. Transmission electron micrograph of a freeze-etched and metal-shadowed bacterial cell (*Desulfotomaculum nigrificans* strain NCIB 8706) revealing an S-layer with square (p4) lattice symmetry on its surface. Bar, 200 nm.

and at interfaces, and summarizes the most recent findings concerning the multistage assembly process.

2. Description of S-layers

2.1. S-layer carrying prokaryotic organisms

S-layers are observed in species of nearly every taxonomical group of walled Gram-positive and Gram-negative bacteria and represent an almost universal feature of archaea (figure 1) [1, 29, 104, 109, 115]. S-layers are monomolecular arrays of a single protein or glycoprotein species (M_w 40 to 200 kDa), and cover the archaeal or bacterial cell completely. However, some organisms exhibit double layers, or more complex S-layer lattices which also consisit of different S-layer proteins as well [29, 115]. If glycosylated, the degree of glycosylation and glycan composition can vary considerably [1, 25, 63]. One of the key features of isolated native and recombinant S-layer proteins is their intrinsic capability to reassemble in suspension and at interfaces (figure 2).

In most archaea, the S-layer is directly attached to the cytoplasmic membrane either by pillar-like, hydrophobic trans-membrane domains, or by modified lipids [1, 115]. In Gram-positive bacteria, the S-layer is often non-covalently bound to hetero polysaccharides (secondary cell wall polymers (SCWPs)) of the peptidoglycan matrix while in Gram-negative bacteria to the lipopolysaccharides (LPS) of the outer membrane of the cell [24].

S-layer proteins are continuously synthesized in the growing cells and translocated to the sites of lattice growth [29, 115]. In most organisms, the rate of synthesis of S-layer protein appears to be strictly controlled since only small amounts are shed into the growth medium. On the other hand, studies on a variety of bacillaceae have demonstrated that a pool of S-layer subunits, at least sufficient for generating one complete S-layer on the cell surface, may be present in the peptidoglycan containing the cell wall matrix [13]. Nevertheless, it has to be stressed that S-layer proteins are produced in larger amounts than any other class of proteins in the cell, and thus are, considering that two-thirds of the biomass on earth belong to prokaryotic organisms, one of the most abundant biopolymers on earth [115].

The dynamic process of the incorporation of new subunits into (closed) S-layer lattices on bacterial cells was studied by electron microscopical labelling experiments [32, 47, 117], and on archael cells by analyses of the number and distribution of lattice faults seen in freeze-etched, metal-shadowed preparations [61, 72, 135]. It was found that the constituent units are incorporated at specific sites, and that the S-layer proteins continuously rearrange themselves during cell growth in order to maintain an equilibrium of lowest free energy [55, 110]. This process requires a pattern-neutral supporting layer allowing free rotation and movement of the subunits to form the regular patterns (e.g. the SCWP) or plasma membrane, and determining the S-layer pattern only by the directional bonds between the protein subunits [102].

2.2. General biochemical properties of S-layer proteins

In general, S-layer proteins exhibit two separated morphological regions, namely a cell wall anchoring and a self-assembly region [8, 27]. Otherwise, homology on the sequence level is low, with the exception of S-layer proteins of certain Gram-positive bacteria whose N-terminal parts, serving as anchoring region at the inner S-layer face, share three ca. 55-amino-acid-long repeats of a surface layer homology (SLH) domain recognized by the SCWP [24, 27, 70]. Accordingly, the C-terminal region is assumed to be located at the outer S-layer face [17, 51, 64, 91].

Most S-layers of bacteria are composed of weakly acidic proteins, contain 40–60% hydrophobic amino acids, and possess few or no sulphur-containing amino acids. The pI values of S-layer proteins range from three to six. For some archaea and lactobacilli, however, pIs of the S-layer proteins have been found between eight and ten [4, 106, 115]. S-layer proteins show high amounts of glutamic and aspartic acid (ca. 15 mol%) and lysine (ca. 10 mol%). Hydrophilic and hydrophobic amino acids do not form clusters. Concerning the surface charge of S-layers in bacillacaea, it was demonstrated that the outer face (with respect to the bacterial cell) is usually charge neutral, whereas the inner one is often net negatively or positively charged, depending on the equity or excess of exposed carboxylic acid or amino groups [33, 88].

Information concerning the secondary structure of S-layer proteins was derived from either circular dichroism measurements [48], Fourier-transform infrared spectroscopy (FTIR) [30], the amino acid sequence using computational approaches [43, 45], or, most recently, from x-ray crystallography studies [6, 70]. In most S-layer proteins, 40% of the amino acids are organized as β-sheets and 10–20% occur as

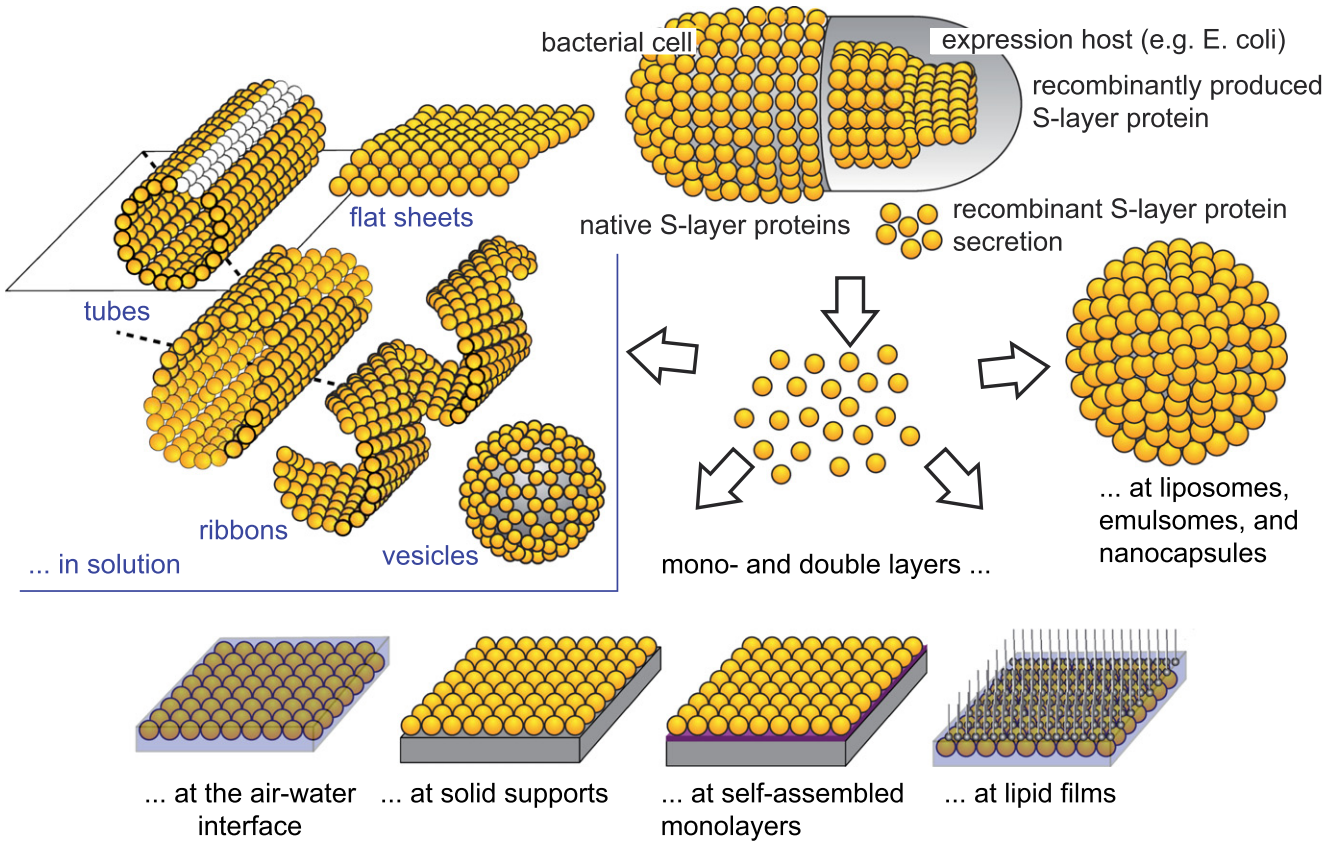

Figure 2. Schematic drawing of the reassembly of S-layer proteins in solution (tubes, ribbons, mono- and double layer sheets), at the air-water interface, lipid films, solid supports, self-assembled monolayers, and at liposomes and polyelectrolyte nanocapsules. The formation of a tube occurs by rolling-up of a flat sheet (top left). This may happen either parallel to a side or to the diagonal (dashed line) of the sheet (modified with permission from [77], copyright MDPI 2013).

α-helices, whereas aperiodic folds and β-turns content may vary by 5–45%. In a new approach, the molecular basis of S-layer protein and metal interactions and their impact on secondary-structure elements were investigated by studying the palladium ($Pd^{(II)}$) coordination in the S-layer protein of *B. sphaericus* strains JG-A12 and NCTC9602 [30]. FTIR revealed ca. 35% β-sheets, little helical structures, a remarkably low pI-value near 3, but, most interestingly, a structural stabilization when $Pd^{(II)}$ is bound [30].

Although several attempts had been made to get three-dimensional (3D) S-layer protein crystals with suitable size from native proteins, it turned out that only genetically modified S-layer proteins (Pavkov *et al* 2008, Fagan *et al* 2009, Kern *et al* 2011, Pavkov-Keller *et al* 2011) [28, 53, 69, 70], and using nanobodies as crystallization chaperones [6], were adequate to break the intrinsic propensity of S-layer proteins to form exclusively two-dimensional (2D) self-assembly products. For a detailed review of the structure of S-layer proteins, see [70]. Moreover, in a seminal work, the importance of Ca^{2+} was demonstrated for the coordination of individual structural domains of the S-layer protein SbsB of *Geobacillus stearothermophilus* PV72/p2 and correspondingly for the lattice formation (see below) [6].

2.3. Ultrastructure

S-layers exhibit only oblique (p1, p2), square (p4), or hexagonal (p3, p6) lattice symmetry [3, 7, 46]. Correspondingly, the S-layer lattice type determines the number of proteins per morphological unit: one, two, three, four, or six. In general, the unit cell dimensions of S-layer lattices range from 3 to 30 nm. S-layers are usually 5 to 20 nm thick, whereas S-layers of archaea reveal a thickness of up to 70 nm and exhibit often a mushroom-like morphology with pillar-like domains anchored to the plasma membrane [115]. S-layers commonly show a smooth topography for the outer face, and more corrugated for the inner (with respect to their orientation at the bacterial cell) [1, 7, 16, 46, 70]. Moreover, S-layer lattices are highly porous protein mesh works (30–70% porosity) with pores of uniform size and morphology in the 2–8 nm range [89].

3. Assembly and morphogenesis

In both, archaea and bacteria, S-layer lattices differ considerably in their susceptibility to isolation from the supporting envelope structure and disruption into monomeric subunits. Generally, S-layers are isolated from cell wall

fragments, which were obtained by breaking up the cells and removing the content, including the cytoplasmic membrane. Most often, hydrogen-bond breaking agents (e.g. guanidine hydrochloride or urea) are used to disintegrate and solubilize the S-layer. For a detailed compilation of protocols, see [96]. Nevertheless, today, recombinant S-layer proteins and S-layer fusion proteins are most often used in the investigations. The isolation of recombinant S-layer proteins from the host system usually follows standard procedures developed for the isolation and purification of inclusion bodies from *E. coli* [49, 51, 96]. In this context, it was recently shown that recombinant S-layer proteins produced in *Bacillus subtilis* were secreted into the culture medium but did not recrystallize on the surface of the cells. Instead, they formed self-assembly products in suspension [50].

3.1. Reattachment of S-layer proteins on bacterial cell surfaces

The development of coherent S-layer lattices on growing Gram-positive cells was also studied by reconstituting isolated S-layer proteins onto the cell surfaces of different bacillaceae from which they had been removed (homologous reattachment) or onto those of other organisms (heterologous reattachment) [102, 103]. In detail, upon dialysis of the disrupting agent (urea or GHCl), the isolated S-layer proteins from *Thermoanaerobacter thermosaccarolyticum* and *Thermoanaerobacter thermohydrosulfurium* reassembled into regular arrays (with square (p4) and hexagonal (p6) lattice symmetry respectively) on the cell walls from which they had been removed. Contrary to the large regular arrays on intact cells, the crystalline patches were much smaller. It was shown that the S-layer proteins from one organism could attach to the cell wall of the other one and form their original patterns again. In addition, when a mixture of both S-layer protein species was supplied, small arrays of both lattice types were formed. These observations clearly demonstrated for the first time that the information for the lattice formation and orientation resides in the proteins themselves and is not affected by the support [102, 103].

These homologous and heterologous S-layer reattachment experiments also led to interesting observations concerning the bonding properties between the individual protein subunits associated in the monomolecular array and to the supporting layer containing peptidoglycan. The square and hexagonal patterns were no longer detectable in freeze-etched or negatively stained preparations of cell walls of both organisms when the pH was lowered to less than 3 (figure 3). The walls had the same granular appearance as the surface of acid-treated intact cells. Interestingly, the acid treatment did not cause any loss of proteins from the cell surface, and the pattern became clearly visible again when the pH was raised to 7. These observations indicate that the subunits of the S-layer are not removed by acid treatment, but rather denature to such an extent that a layer with a random granular structure is formed [103]. Considering current knowledge about lectin-type binding involving the SLH domain of the S-layer protein and the SCWP, these data corroborate the observation that the S-layer–SCWP interaction has a stabilizing effect on the conformation of the SLH domain (N-terminal part) of the S-layer protein [83].

3.2. Reassembly in bulk solution

Most *in vitro* self-assembly studies have been performed with S-layer proteins derived from Gram-positive bacteria [110, 114]. Self-assembly products are formed in solutions of S-layer proteins during the dialysis of the disrupting agent against selected buffer solutions (ionic strength and pH) [96, 107]. The monitoring of the time-course of self-assembly by concentration-dependent light scattering yielded multiphasic kinetics with a rapid initial phase and slow consecutive processes of higher than second-order [52, 120]. The rapid phase may be attributed to the formation of oligomeric precursor patches, which act as nucleation sites for consecutive crystal growth (see below as well). Recently, data from kinetic measurements at different temperatures indicated that the assembly process is entropy-driven [120]. It is accompanied by a release of entropically disfavoured water molecules in the hydration layer surrounding the hydrophobic domains of the S-layer protein, and a correspondingly net loss of hydrophobic surfaces in the assembled S-layer lattice (Teixeira *et al*, 2010).

Depending on the morphology and bonding properties of the S-layer proteins, either flat mono- or double layered sheets, ribbon-like morphologies, open-ended tubes, or screw-dislocations are formed (figure 4) [11, 62, 110, 114]. Further on, it was also observed that closed vesicles may be formed by S-layer proteins recrystallizing in hexagonal lattice symmetry [103]. In some cases, it was possible to control the self-assembly routes by changing the environmental conditions such as pH, or ionic content and strength of the subphase. In this context, one of the S-layer self-assembly systems studied in the most detail is the one of SgsE from *Geobacillus stearothermophilus* strain NRS 2004/3a, exhibiting oblique (p2) lattice symmetry with base vector lengths of a = 11.6 nm, b = 7.4 nm, and a base angle of 78° respectively [62, 68, 110]. Depending on the buffer system (its pH, ionic content, and strength), during dialysis and dialysis duration the isolated proteins assembled into both flat and cylindrical mono- and double layer self-assembly products of distinct sizes (figure 4(a)). Sheets and medium (~220 nm in diameter) to large (~1 μm in diameter) cylinders were always double layered in back-to-back orientation and could be classified according to their angular displacement into five different superposition types. The respective superposition types could explain the different diameters of the cylinders, since one of the two layers had to bend against its natural curvature and thus hindered to some extent the roll-up of S-layer sheets. While the small diameter cylinders (~70 nm and ~100 nm, in two classes) were always composed of monolayers, with an intrinsic tendency to roll-up, the formation of the medium- and large-diameter double layered cylinders seemed to be merely resulting from the fact that flat sheets having reached a certain critical size had enough flexibility to curve over, so that by chance opposite edges of the sheet met and subsequently fused (figure 2, top left) [62]. In this context, recently,

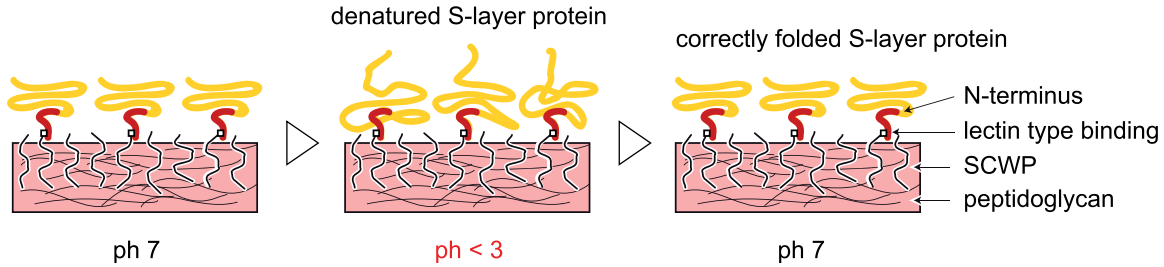

Figure 3. Schematic drawing. The ultrastructure of the S-layer proteins was no longer detectable in freeze-etched or negatively stained cell wall preparations when the pH was lowered from 7 to less than 3. The S-layer protein remained attached to the surface due to the specific lectin type binding with the SCWP. Upon raising the pH to 7 again, the protein was refolded into the correct conformation and the regular pattern became clearly visible again (drawn after [103] description). Adapted with permission from [116]. Copyright 2011 Elsevier.

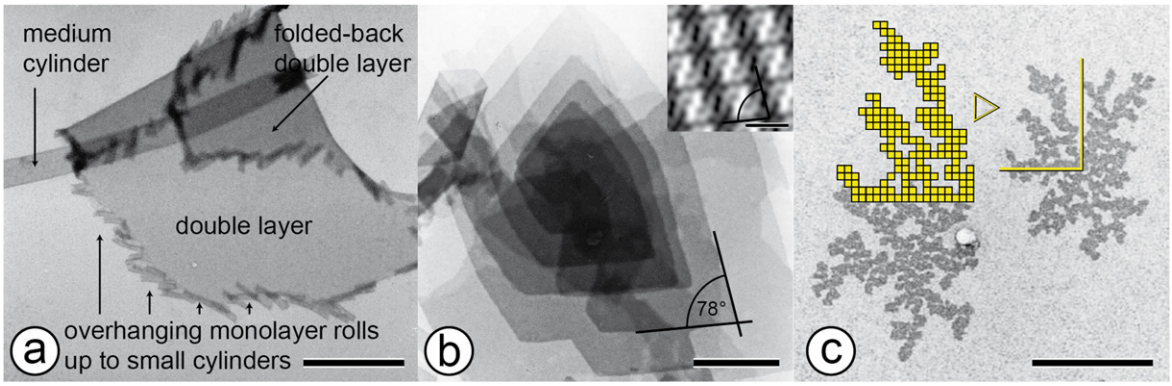

Figure 4. TEM images of (a) and (b) various self-assembly products of the S-layer protein SgsE from *Geobacillus stearothermophilus* NRS 2004/3a [62, 68]. (a) Double layer sheet and double layer medium sized cylinder. At the edge of the incomplete double layer sheet one of the constituent overhanging monolayers rolls up into small diameter cylinders. Bar, 1 μm. (b) Screw dislocation formed in the course of the S-layer lattice formation. The polygonal sheet resembles the base angle (78°) of the S-layer lattice. Bar, 2 μm. Inset: Digital image reconstruction of the S-layer lattice. According to the oblique (p2) lattice symmetry, one morphological unit contains two proteins. Bar, 10 nm. (c) TEM image of tenuous S-layer clusters obtained with the S-layer protein SbpA from *Lysinibacillus sphaericus* CCM2177 upon recrystallization at the air-water interface with no calcium in the subphase. Reprinted with permission from [74]. Copyright 1995 Elsevier. Bar, 1 μm. Inset: Schematic drawing showing that all morphological units in the cluster have the same rotational orientation and no displacements against each other.

the formation of cylindrical self-assembly products was studied for the S-layer proteins from *Geobacillus stearothermophilus* ATCC 12980 and, in great detail, from *Bacillus sphaericus* NCTC 9602 too [11]. Based on experimental studies on tube formation during the self-assembly process, the process parameters which are essential for controlling the particular tube geometry, tube radius, and growth velocity were explored and a mechanistic model describing the underlying details was proposed. It was shown that the tube formation was determined by changes in pH, ionic strength, and the presence of divalent cations (e.g. Ca^{2+} or Mg^{2+}), and by the initial monomer concentration. The S-layer was modelled computationally as a curved sheet with discrete binding sites for the monomer binding and the pathways of protein reassembly described by an interplay of non-specific and specific interactions [132]. In addition, the controlled manipulation of the tube radii by genetic modifications of the S-layer protein indicated that the tube radius is an intrinsic structure parameter [11].

Screw dislocations were obtained upon stirring the S-layer protein solution during dialysis. The probability is that a point defect hinders the isotropic crystal growth, and eventually the S-layer lattice grows along a helical path around the defect (figure 4(b)).

The S-layer protein SbpA of *Lysinibacillus sphaericus* CCM2177 is currently one of the most studied model systems [15, 17, 43, 51, 67, 73, 74, 100, 101]. SbpA shows square (p4) lattice symmetry with a lattice spacing of a = 13.1 nm. The gradual truncation of SbpA, with a full length of 1268 amino acids (including a 30-amino-acid-long signal peptide), led to an unexpected result [48]. It was found that a deletion of 200 C-terminal amino acids (yielding $SbpA_{31-1068}$) did not hinder the self-assembly properties of the protein, and left the ultrastructure and lattice parameters unchanged. However, upon a further truncation of the amino acid sequence, leading to $rSpbA_{31-918}$, an S-layer lattice was formed with oblique (p1) lattice symmetry and base-vector lengths of a = 10.4 nm and b = 7.9 nm respectively and a base angle of 81°. It is interesting to note that—at a resolution of ~1.5 nm in negatively stained preparations—the ultrastructure of this newly formed S-layer lattice looked identical to that of SbsB, the S-layer protein of *Geobacillus stearothermophilus* PV72/p2

[56, 64], and to that of the physiologically induced strain *G. stearothermophilus* NRS 2004/3a variant 1 (V1) [87]. For comparison, the mature $SbsB_{32-920}$ was only one amino acid longer than $rSbpA_{31-918}$. Both S-layer proteins carry three SLH-motifs on the N-terminal part which showed high identity. But no sequence similarities were found for the middle and C-terminal parts. Finally, further C-terminal truncation of $rSbpA_{31-918}$ led to a complete loss of the self-assembly properties of the S-layer protein [48]. Unfortunately, no data are available concerning the amino acid sequence of *G. Stearothermophilus* NRS 2004/3a variant 1 (V1). Nevertheless, it may be speculated that the structure of the truncated protein that reassembles into a lattice with oblique (p1) lattice symmetry constitutes a *minimal*, *common molecular unit* fulfilling diverse functional requirements for an S-layer protein of these organisms. Further work will be necessary to elucidate these findings in detail.

3.3. Assembly at the air-water interface and at Langmuir-Blodgett monolayers

Two decades ago, investigations concerning the specific interactions of S-layers with molecules, cells, and surfaces led to the development of protocols for generating extended S-layer protein monolayers at various interfaces. As a first step, a simple strategy was developed for the reassembly of S-layer proteins at the air-water interface and at phospholipid monolayers (spread on a Langmuir-Blodgett (LB) trough) [73, 78]. This approach was intriguing since it had already been assumed that S-layers might also be used as supporting and stabilizing structures for LB-films and reconstituted biological membranes [107]. Such composite structures would not only mimic the molecular architecture of archaeal cell envelopes, which are exclusively composed of an S-layer and a plasma membrane, but would also lead to new techniques for exploiting structural and functional principles of membrane associated and integrated molecules. All these assumptions came true in the following years (for review see [92, 93, 95]). The first experiments were performed with the S-layer protein from *Bacillus coagulans* E38-66 [88]. This S-layer protein shows oblique (p2) lattice symmetry with base vector lengths of a = 9.4 nm, b = 7.4 nm, and a base angle of 80°. Because of the asymmetry in the physicochemical surface properties of this S-layer protein and the clearly discernible orientation of the oblique lattice, it could be unambiguously concluded that they were oriented with their outer face (with respect to the bacterial cell) against the air-water interface and with their negatively charged inner face to the zwitterionic head groups of spread dipalmitoylphosphatidylcholine (DPPC) and dipalmitoylphosphatidylethanolamine (DPPE) monolayer films. In addition, and for the first time, the dynamic S-layer crystal growth could be (indirectly) shown by transmission electron microscopy (TEM). For this purpose, S-layers and composite S-layer-lipid films were transferred onto electron microscope grids which had been carefully placed on the liquid surface before and then removed by horizontal lifting (referred to as Langmuir-Schaefer technique in the literature [124]) at certain time intervals (after 20, 40, and 60 min) [78]. It was found that crystal growth was initiated at several distant nucleation points and proceeded in plane until the front regions of neighbouring crystalline areas met, resulting in a closed mosaic of crystalline domains, typically 2–10 μm in diameter. This general model of S-layer lattice formation was recently reinvestigated in detail by *in situ* high resolution atomic force microscopy (AFM) and refined towards a description as a non-classical, multistage crystallization pathway [15] (see next section for details). An optional cross-linking step using glutaraldehyde, which was injected into the subphase after completion of the S-layer lattice formation, considerably increased the mechanical stability of the layered structures for subsequent handling procedures [78].

Further on, the reassembly of S-layer proteins at the air-water interface and at lipid films was investigated by using the S-layer protein SbpA as the model system. SbpA forms extended monolayers consisting of coherent crystalline domains up to 10 μm in diameter at lipid monolayers, bilayers, and tetraether lipid films (pH 9) (figures 5(a)–(d)) [73, 74]. It has to be noted that after prolonged periods of time, double layers are formed too. By comparing the surface topography of freeze-dried incomplete mono- and double layer patches with that seen in freeze-etched preparations of whole cells, it was concluded that the two layers were facing each other with their net negatively charged inner faces (concerning the orientation at the bacterial cell). TEM studies showed that S-layer-supported lipid membranes may cover holes (up to 10 μm in diameter) in holey carbon films and, most relevant for technological approaches, apertures in microfabricated silicon discs [73]. Further on, it was assumed that the amount of lipid molecules in the monolayer bound to the S-layer lattice modulates the lateral diffusion of the remaining free lipid molecules and consequently the fluidity of the whole membrane; thus the term *semifluid membrane* was coined [73]. Later, fluorescence recovery after photobleaching (FRAP) showed the validity of this assumption [34], and the increase in lifetime and robustness of S-layer-supported lipid membranes (phosphor- and tetraether lipids) was further investigated and exploited [93, 95, 127, 128]. Compared to lipid monolayers on alkylsilanes and lipid bilayers on dextran cushions, S-layer-supported lipid bilayers revealed the highest mobility of the lipid molecules [34]. S-layers recrystallized on both sides of lipid bilayers increased the transversal motion of the lipid molecules compared to unsupported lipid layers (figure 5(d)) [42, 94].

In this context, in a layered lipid-protein membrane architecture, the reciprocal influence between S-layer protein from *B. coagulans* E38-66 and two lipid components, DMPE (dimyristoylphosphatidylethanolamine) and DPPE, was investigated by dual-label fluorescence microscopy, FTIR, and TEM [21]. It was found that the phase state of the lipid had a strong influence on S-layer protein reassembly. When the lipid monolayer was in a phase-separated state between the solid and fluid phase, the S-layer protein nucleated at the boundary lines between the coexisting lipid phases, and recrystallization proceeded preferentially underneath the fluid phase. Further on, FTIR showed that the S-layer protein

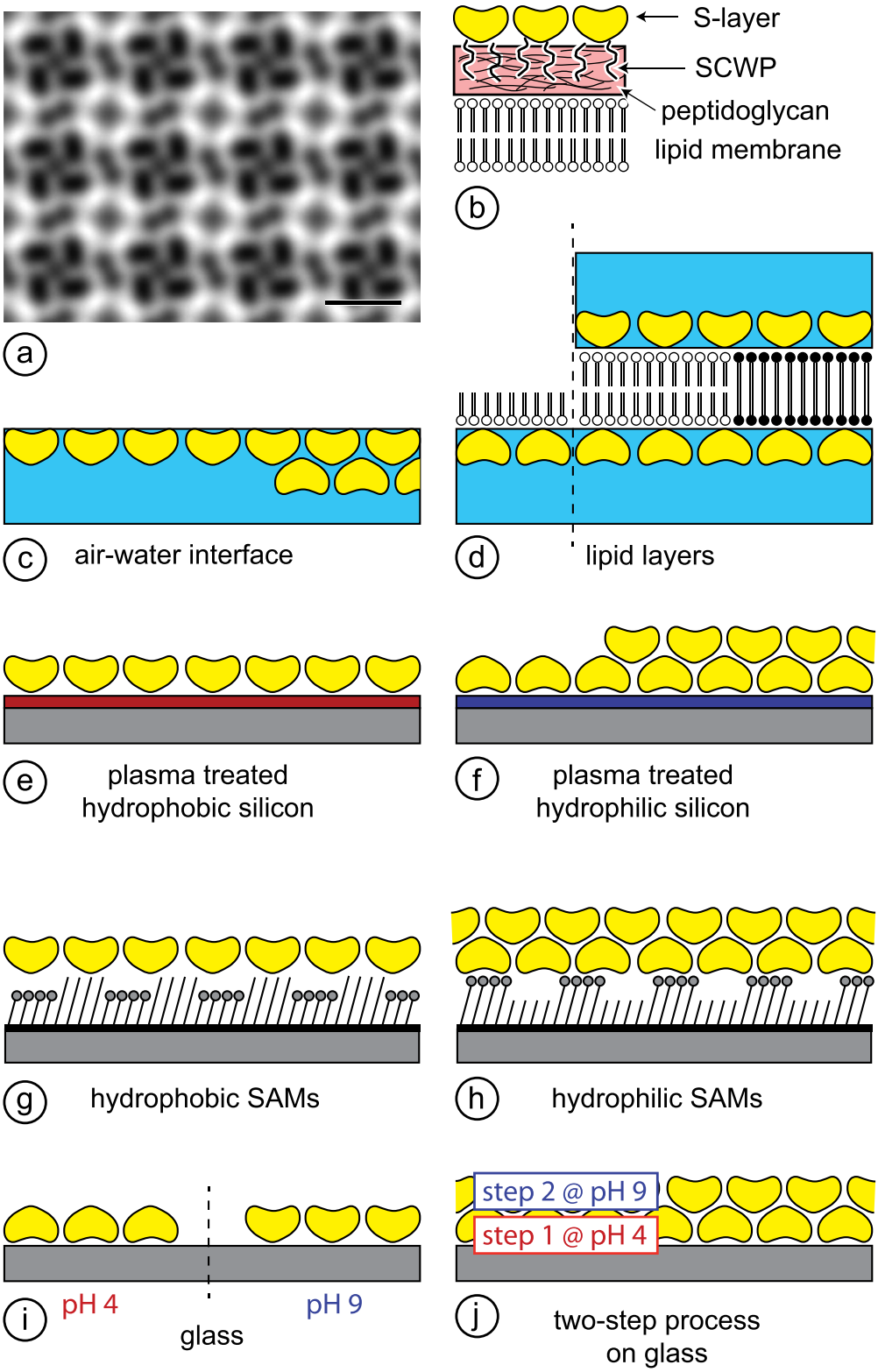

Figure 5. (a) TEM image of the ultrastructure of the S-layer protein SbpA from *Lysinibacillus sphaericus* CCM2177 [51]. The image was obtained from a negatively stained preparation of an SbpA monolayer after enhancing the signal-to-noise ratio by Fourier domain filtering [73]. Bar, 10 nm. Schematic drawing of (b) the Gram-positive bacterial cell wall profile of *L sphaericus* CCM2177 with the S-layer proteins anchored through SCWPs, and the reassembly at (c) the air-water interface, (d) at phospholipid monolayers (left), bilayers, and tetraether lipid monolayers generated by black lipid membrane procedures (right) [73, 74], on silicon surfaces rendered (e) hydrophobic or (f) hydrophilic by plasma treatment [33], on (g) hydrophobic and (h) hydrophilic solid supported SAMs [65], and (i) and (j) on glass (contact angle 56 ± 4°), depending on the pH value [81]. In a two-step process, in which the reassembly is performed first at pH 4 and subsequently at pH 9, double layers are formed (pI of SbpA 4.6) [81]. Adapted with permission from [116]. Copyright 2011 Elsevier.

assembly affected the order of the alkane chains and brought the fluid phase into a state of higher order. Surface-sensitive scattering techniques (grazing-incidence x-ray diffraction as well as x-ray and neutron reflectometry studies) confirmed theses findings not only for the S-layer lattice from *B. coagulans* E38-66 with its oblique (p2), but also for the S-layer lattice of SbpA with its square (p4) lattice symmetry [129–131]. A comparison of the monolayer structures before and after protein recrystallization showed minimal reorganization of the lipid chains but, in contrast, a major reorientation of the lipid head groups towards the surface normal. For the reassembly of SbpA S-layer proteins at DPPE monolayers, x-ray reflectivity data suggested that the amino acid side chains intercalated the lipid head groups at least to the phosphate moieties, and probably further beyond [129–131].

In another study, concerning the reassembly of S-layer protein from *B. coagulans* E38–66 at different phospholipid monolayers, it was confirmed that the nature of the lipid head groups, the phase state of the surface monolayer, the ionic content, and the pH of the subphase are the most important parameters for S-layer lattice formation [127]. S-layer lattices covered the whole sample area (in the presence of Ca^{++}) when the head groups were zwitterionic and the monolayer was in (or close to) its solid state. In this case, the S-layer proteins were attached to the lipid film with their net negatively charged inner face (with respect to their orientation towards the bacterial cell). In contrast, although the S-layer protein adsorbed under most lipids with negatively charged head groups and under lipids with unsaturated chains (as determined by an increase in surface pressure), they did not form crystalline domains. At positively charged lipid head groups, the S-layer proteins reassembled into monolayers with their outer face (with respect to the bacterial cell) oriented towards the interface.

The importance of the calcium concentration (in the subphase) for the reassembly of SbpA was shown for the first time by studying the anisotropic crystal growth at the air-water interface (figure 4(c)) [74]. In general, calcium—as divalent ions—may bind to specific sites of the protein domains, thereby modifying the crystal structure, and/or being directly responsible for protein interactions (as shown for SbsB in [6]). Depending on the calcium concentration, a broad spectrum of crystal morphologies ranging from tenuous, fractal-like structures, to micrometer-sized mono crystalline patches were found. Although all structures looked like fractals obtained by diffusion-limited aggregation, they were not aggregates of randomly oriented proteins. Digital image processing showed that all morphological units in the cluster had the same rotational orientation and no displacements against each other (inset in figure 4(c)). Although the shape of the clusters was irregular, they showed perfect square (p4) lattice symmetry on the molecular level. The observed S-layer clusters were not fractals since they did not show scaling symmetry (scale invariance) [84]. The shape of the structures was more reminiscent of a dense branch morphology (DBM) [9]. A characteristic feature of DBM is tip splitting, which distinguishes these structures from dendrites. No significant differences in the shape of the clusters were found when the recrystallization time was extended from 12 to 48 h. Only the holes in the clusters were filled. From these data it was concluded that S-layer crystal formation is determined at the air-water interface by a fast nucleation and assembly of subunits already at the air-water interface and a slow incorporation from the subphase.

3.4. Assembly at inorganic surfaces, solid supported lipid monolayers, and self-assembled monolayers (SAMs)

Currently, a great variety of supports, differing in their physicochemical properties, are being investigated in order to meet new (nano)technological demands. Silicon, mica, and metal surfaces are exploited for applications in nano electronics, glasses in nano optics, and polymeric surfaces, e.g. SU-8 resist, in microfluidics [71, 81]. As a matter of fact, AFM is most often used to study the reassembly of S-layer proteins on solid supports [15, 23, 36, 55, 65, 75, 101, 119], while in TEM studies, composite thin film/carbon-coated electron microscope grids (EM-grids) and, most recently, graphene are used [17, 80].

In most cases, the surface has to be rendered hydrophilic or hydrophobic by plasma treatment before use. For example, as shown by *in situ* AFM, the S-layer protein SbpA forms monolayers on hydrophobic (figure 5(e)) and double layers on hydrophilic silicon surfaces, both in the presence of Ca^{2+} (pH 9) (figure 5(f)) [36, 55]. It was found that, in comparison to hydrophilic surfaces, the layer formation was faster on hydrophobic supports (30 min versus 60 min for full coverage). Crystal formation started from many different nucleation sites leading to a mosaic of small crystalline domains which were less than 200 nm in diameter on average [75]. The size of the crystalline domains on oxygen plasma-treated hydrophilic surfaces was much larger, with mean diameters of 2–10 μm. According to the observation of the reassembly at the air-water interface and on LB films [73, 78], crystal growth was initiated at several distant nucleation points and proceeded on the surface until the growing crystalline domains met. It must be stressed that the formation of larger domains was favoured at low monomer concentrations due to the corresponding lower number of nucleation sites, and that no overlapping regions or seams along the grain boundaries were found [55, 120]. In addition, rupture of the S-layer lattice with the metal chelator ethylenediaminetetraacetic acid (EDTA) confirmed the importance of the divalent calcium ions in the layer formation [36].

In a further experimental study, the effect of the hydrophobicity of the support was investigated by studying the SbpA reassembly on SAMs on gold. The SAMs were composed of disulfides with different end groups (OH versus CH_3) and lengths of the individual methylene chains [65]. Formation of monolayers was observed when the hydrophobic end groups (CH_3) surmounted the hydrophilic (OH) groups (figure 5(g)). Conversely, double layers were formed when the hydrophilic (OH) groups superseded the hydrophobic (CH_3) end groups (figure 5(h)). The threshold for the transition in the hydrophobicity/hydrophilicity was only four methylene groups. Moreover, beside the formation of mono-

versus double layer assemblies, the lattice parameters (base vectors and layer thicknesses) changed from $a \simeq 15.6$ nm and $d \simeq 8.6$ nm for the hydrophobic to $a \simeq 12.7$ nm and $d \simeq 15.2$ nm for the hydrophilic surface [65].

The silanization of a silicon or glass support with either aminopropyltriethoxysilane (APTS) or octadecyltrichlorosilane (OTS) is also often used to render the surface properties hydrophobic [55]. On such silanized surfaces, the reassembly of the S-layer protein SbpA was investigated by combining the results from AFM with those from a quartz crystal microbalance with dissipation (QCM-D) studies. It was shown that a full S-layer protein coverage on APTS- and OTS-modified surfaces may be obtained within 2–3 h, whereas it took more than 12 h on a native silicon dioxide surface rendered hydrophilic by plasma treatment [55]. The crystalline domains were much smaller on silanized substrates ($\sim 0.02\,\mu m^2$ for APTS and $\sim 0.05\,\mu m^2$ for OTS) compared to hydrophilic silicon dioxide ($\sim 32\,\mu m^2$). Finally, the study concluded that S-layer formation occurs in three consecutive steps: (i) diffusion-controlled protein adsorption with a threshold concentration of 0.05 mg mL^{-1} at APTS and OTS, and 0.07 mg mL^{-1} on silicon dioxide); (ii) self-assembly by incorporation of proteins at domain boundaries; and (iii) reorganization of neighbouring crystalline domains into bigger ones [55].

Most recently, the anisotropy between the inner and outer S-layer face of the S-layer protein SbpA was used to develop a novel, tuneable, facile, and reliable method for cellular micropatterning [81]. By simply altering the recrystallization protocol from basic (pH 9) to acidic (pH 4) conditions, the SbpA S-layer orientation was adjusted to effectively prevent protein adsorption and cell adhesion (smooth outer cytophobic side exposed), or, alternatively, to promote cell attachment and spreading (rough inner cytophilic side exposed) (pI of SbpA is 4.6) (figure 5(i)). It must be noted here that the recrystallization of SbpA is usually carried out at pH 9. Further on, in a controlled layer-by-layer approach, starting with a recrystallization at pH 4 followed by a second step at pH 9, a double layer was formed with the two constituent monolayers facing each other with their inner cytophilic sides (figure 5(j)).

Recently, the general picture of S-layer crystal growth at interfaces was significantly improved by high resolution *in situ* AFM and computational simulations of the individual stages in the lattice formation of SbpA from *Lysinibacillus sphaericus* ATCC 4525 (identical to *L. sphaericus* CCM2177 [70]). The investigations were performed by AFM on solid supported self-assembled monolayers consisting of 1-palmitoyl-2-oleol-sn-glycero-3 phosphocholine (POPC) (deposited on mica) [15], on mica [101], and by Cryo-TEM and tomography on graphene [17]. It turned out that the assembly process is multistage and correlated to conformational changes that direct the non-classical pathway of assembly. First, extended monomers (height ca. 2 nm) were adsorbed onto the lipid surface where they condensed into amorphous clusters (pH 7.1) [15]. After the surface was densely populated with adsorbed protein, amorphous clusters with nearly uniform height (ca. 10 nm) were formed. After this extended incubation period (ca. 80 min), the clusters gradually began to show internal ordering and finally, after 5 to 10 min, transformed into crystalline arrays of compact tetramers exhibiting square (p4) lattice symmetry (height ca. 10 nm) [15]. Finally, crystal growth proceeded by the incorporation of new subunits at the edge sites of the lattice. Lattice growth is autocatalytic since it can be shown that the activation energy, associated with the creation of new tetramers, is only half of the free-energy barrier for folding of a single monomer [15]. Thus, the conformational transformation of the monomer to the oligomeric form is an inherent part of the assembly process! The rate-limiting step is the closure of the incomplete morphological unit (consisting of three subunits only) by adding the last monomer [17]. This last S-layer protein is locked in place, and since it was never observed that S-layer proteins leave the formed lattice, it was concluded that lattice growth is irreversible and the state of lowest free energy is obtained [15, 17].

In this context of elucidating the non-classical pathway of matrix assembly of S-layer proteins [18], it was also demonstrated that on bare mica a kinetic trap associated with conformational differences between a long-lived transient state and a final stable state (along a folding funnel [22]) plays an important role. Both ordered tetrameric states emerged from clusters of the monomers but developed along two different pathways. While the final stable conformation was directly obtained, the trapped transient state—characterized by reduced height—transformed only over time to its final low-energy state. Careful analysis of the time and temperature dependence of formation and transformation yielded an energy difference by only 1.6 kJ mol^{-1} (or 0.7 kT). However, the energy barrier to transforming into the final low energy state was 61 kJ mol^{-1} and hence 38 times higher.

Nevertheless, in summarizing the detailed knowledge gained in the *in situ* AFM experiments with SbpA described above, the question concerning the formation of the very first morphological unit, for SbpA the first tetramer, remains challenging. Moreover, it is most interesting to know (or estimate) how many monomeric units constitute a nucleation site with sufficient internal order to initiate lattice growth along the formed domain. Concentration-dependent dynamic light scattering (DLS) measurements gave evidence for a 'critical concentration' of association in the range of 12–16 monomers for the S-layer protein of *B. stearothermophilus* NRS 1536/3a (showing square (p4) lattice symmetry) [52], and an intensity-weighted Z-average diameter for the ensemble collection of particles of 75 nm for SbpA (ca. 20–25 monomers) [120]. Accordingly, *in situ* AFM, in combination with a computational approach, showed initial cluster sizes of 2–15 tetramers, corresponding to 8–60 monomers, from which crystal growth proceeded as described before [15]. Although high resolution *in situ* AFM images were captured, the impact of the scanning AFM tip on the assembly of the first individual monomers is not negligible, and thus it is difficult to give a good estimate of the minimum number of monomers for a nucleation site by experimental means only. In a theoretical approach, the formation of an S-layer lattice with p4 lattice symmetry (as for SbpA) was investigated by

assuming both non-specific attractive and specific directional bonds for the monomers [41, 132]. The results were in very good agreement with the experimental findings, by showing, for example, that liquid-like clustering may precede crystallization. Moreover, since S-layer lattice types range from p1 to p6, and correspondingly different numbers of proteins constitute one morphological unit (unit cell), the question has to be addressed to different lattice symmetries as well. In particular, the oblique (p1) lattice symmetry is challenging because the morphological unit comprises a single monomer only. Major insights on the mechanism of S-layer formation were recently obtained after elucidating the crystal structure and the importance of Ca^{2+} for SbsB [6]. Ca^{2+} triggers a conformational change of the SbsB monomer from an extended to a φ-shaped assembly-competent structure. While the main intramolecular contact points stabilizing the monomer are between domains IV and VII, the interactions between neighbouring subunits in the oblique lattice occur between domain II and IV. Since the bonding pattern in this particular S-layer lattice in known now, it might be used for developing a growth model using realistic parameters. Anyway, the lattice formation for SbsB was simulated using a coarse-grain model for the monomers, in a Monte-Carlo study, but in fact could not take into account such minute information—such as the involvement and location of particular structural domains [44]. Nevertheless, it has to be stressed that theoretical work has already supplied extremely valuable information concerning the crucial question about the event leading to the spontaneous formation of nucleation sites [121].

3.5. Reassembly on biopolymers, polyelectrolyte layers, and charged surfaces

S-layer proteins have a high affinity to biopolymers (e.g. polylysine, polyarginine) and in particular, in the case of Gram-positive bacteria, to their corresponding SCWPs by specific carbohydrate-protein interactions [48, 56, 85, 86, 113]. According to the orientation on the bacterial cell, S-layer proteins assemble on SCWP-coated supports with their inner faces (N-terminus), and thus expose their outer faces (C-terminus) towards the environment (figure 6). This property is especially important for functionalizing surfaces with C-terminal S-layer fusion proteins, since it is then ensured that the introduced functionality is exposed towards the environment [49, 64, 115].

Further on, the reassembly of S-layer proteins on negatively and positively charged polyelectrolyte layers was investigated too, in order to discover whether the orientation of the S-layer lattice may be controlled in this way. For this purpose, the reassembly was studied of SbpA and of SbpA-green fluorescent fusion protein (rSbpA-EGFP) on flat polymer coated substrates and on nanocapsules [19, 20, 122]. Different polyelectrolytes were used, such as the anionic poly-sodium 4-styrenesulfonate (PSS), poly-acrylicacid (PAA), and the cationic poly-ethylenimine (PEI, used as precursor in the layer-by-layer technique only), poly-allylamine hydrochloride (PAH), and poly-diallyldimethyl

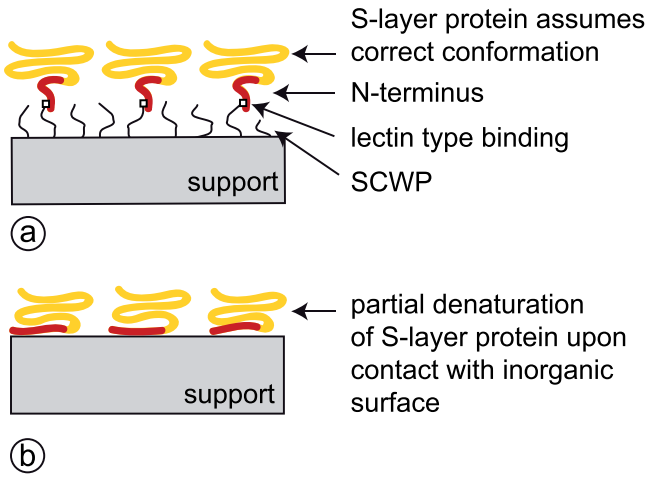

Figure 6. (a) S-layer proteins reassemble on biomimetic SCWP-coated surfaces with their correct conformation. SCWP recognizes and stabilizes the N-terminal part of the S-layer structure. (b) On plain inorganic supports (gold, SiO_2, etc) it is most likely that the protein denatures partially upon contact with the surface.

ammonium chloride (PDADMAC). The layer-by-layer technique was applied to generate the polyelectrolyte multilayers: $PEI/(PSS/PAH)_6$, $PEI/(PSS/PAH)_6/PSS$, $(PAA/PDADMAC)_3/PAA$, and $(PAA/PDADMAC)_3$. Successful S-layer reassembly with micrometer-sized coherent crystalline domains could be achieved in the presence of divalent cations (Ca^{2+} or Mg^{2+}) on the negatively terminated polyelectrolytes PSS and PAA. Both polyelectrolytes mimic to a certain extent the (negatively charged) SCWP of *L. sphaericus* CCM2177 [51]. Reassembly of SbpA on positively charged polyelectrolyte PAH leads only to small crystalline patches, while larger arrays could be achieved, surprisingly, on strongly positively charged PDADMAC terminated layers. In both cases, the S-layer was attached with its outer charge neutral face against the polyelectrolyte layer. In a subsequent work, novel hybrid sandwich-like supramolecular structures were built composed of polyelectrolyte/S-layer/polyelectrolyte/ (S-layer) [20]. Neutron reflectometry studies confirmed the successful reassembly of SbpA on PSS, and, in combination with QCM-D studies, permitted the calculation of the S-layer density (*ca.* $1.16\,g\cdot cm^{-3}$) and an estimate of the amount of bound water. It was concluded that SbpA forms a loose layer on anionic PSS incorporating a water volume fraction of about 68%.

In addition to the reassembly experiments on charged polyelectrolyte coated surfaces, the influence of the (electrical) charging state of the substrate on the S-layer protein reassembly was investigated by studying the electrochemical behaviour of SbpA S-layer proteins on potentiostatically controlled gold electrodes [38, 112]. It was shown by AFM that in the positively charged electrochemical double layer region—with anion excess positive of the point of zero charge (ca. −800 mV versus a saturated mercury-mercurous sulphate electrode)—the negatively charged binding sites of the S-layer proteins (e.g. carboxylates) could bind to the positively charged gold surface atoms and form homogenous

polycrystalline monolayers. In contrast, in the negatively charged electrochemical double layer region (with cation excess negative of the point of zero charge), isolated multilayer clusters of S-layer proteins arranged themselves around a few nucleation sites. Unfortunately, the resolution in AFM images obtained did not allow us to distinguish between inner and outer S-layer face (with respect to the orientation at the bacterial cell). Time-resolved *in situ* electrochemical quartz microbalance investigations and *ex situ* small-spot x-ray photoelectron spectroscopy (XPS) measurements demonstrated that the 2D S-layer crystal formation depends on the potential of the gold electrode and on the presence of (linking) Ca^{2+} ions, and can be ideally achieved within minutes.

3.6. Reassembly at liposomes, emulsomes, and nanocapsules

Liposomes, emulsomes, and nanocapsules are often used as model systems for studying biological membranes and as delivery systems for biologically active molecules [54, 58, 122, 123]. S-layers reassembled on the curved surfaces show numerous lattice faults (edge dislocations and disclinations), which are a necessity for rigid layers to completely cover spherical bodies [39, 40, 66]. The orientation of the S-layer is determined by the surface charge of the used lipids or polyelectrolytes as described for the reassembly at planar lipid membranes or polyelectrolyte layers. Extensive studies with S-layer coated liposomes have demonstrated that the S-layer lattices enhance the stability of the liposomes against mechanical stresses (exerted by shear forces or ultra sonication), against thermal challenges, and changes in zeta-potential. These findings are important for nanomedical applications like drug targeting and delivery [54, 57, 58]. Furthermore, S-layer liposomes resemble the supramolecular envelope principle of a great variety of human and animal viruses and, thus, will allow the investigation of artificial viruses, as discussed for gene therapy [2, 115].

4. Conclusion and perspectives

Basic research on the structure, genetics, chemistry, morphogenesis, and function of S-layers has explicitly demonstrated that they are the simplest biological protein membranes developed during evolution. A profound understanding of the basic mechanisms and parameters in the reassembly of S-layer proteins, the directed control of the lattice orientation in such a way that functional groups and domains are exposed to the environment, or the spatial constriction of the S-layer lattice formation by micro-lithographically-based methods, for example by micromoulding in capillaries (MIMIC) [35, 81], was of fundamental importance for the introduction of S-layer proteins as molecular building blocks in both the life and non-life sciences [105, 106, 115, 116]. Although a considerable amount of knowledge has already been accumulated with native S-layer proteins, a major breakthrough was achieved by the design and expression of specific S-layer fusion proteins for a broad range of applications [24, 49]. The possibilities are numerous but share the common properties of S-layers such as selectable lattice constants, isoporosity, antifouling characteristics, or molecular precision in the control over surface properties by chemical or genetic modifications. Examples are the development of S-layer ultrafiltration membranes characterized by their precisely defined cut-off characteristics [89, 90, 109], or the excellent antifouling properties of S-layers, recently brought to a new application in microfluidics and cellular micropatterning by controlling cell adhesion or repulsion via their orientation against the substrate [71, 81]. The development of S-layer fusion proteins with specifically tailored functionalities, such as the major birch pollen allergen or the ZZ domain (IgG binding domain of protein A) [12, 51, 115], opened a new horizon in the development of novel affinity matrices. In addition, the use of a bottom-up approach based on S-layers as templates in the formation of perfectly-ordered nanoparticle arrays was completely new in the field of nano electronics and optics and opened for the first time a fabrication technology for the self-assembly of nanometre scale metallic islands [10, 37, 59, 60, 76, 79, 99, 126]. Moreover, the implementation of S-layers as stabilizing nanostructures in the development of solid supported and free-standing functional lipid membranes is entirely new in the field of membrane research [92, 93, 95]. This construction principle mimics the archaeal cell envelope structure which has been optimized over ~3.5 billions of years under extreme environmental conditions (e.g. 120 °C; pH 0; concentrated salt solutions; 1100 bar) [1]. The technology of S-layer stabilized lipid membranes has the potential to initiate a broad range of developments in many areas, such as diagnostics, high-throughput screening for drug discovery, membrane-based protein-based sensor technology, electronic and optical devices, and even DNA sequencing [95, 111, 115]. In this context, it is important to remember that 60% of consumed drugs act on membrane proteins. S-layer coated liposomes and emulsomes have also gained broad interest in the scientific community since they provide nano containers with high mechanical and thermal stability, allow addressor molecules to bind, demonstrate a novel possibility for the transport of hydrophilic and hydrophobic substances, and allow the development of artificial viruses [54, 57, 58, 123]. In this context, based on the experience of coating liposomes with S-layer proteins and using them as templates in the biomineralisation of silica, a new generation of chemically inert hollow nano containers has been developed [31, 97]. In comparison to virus capsids (typically 30–100 nm in diameter) or hollow (apo)ferritin (12 nm in diameter), S-layer cages may be much larger and adjustable in size. We can anticipate that S-layers will continue to have great impact as patterning elements and as parts of a toolkit in the development of novel applications in bionanotechnology, biomimetics, and synthetic biology.

It must be stressed that the most obvious deviation from the classical pathways of nucleation and crystal growth is the observation that S-layer protein folding is directly linked with protein assembly into extended clusters. In this multistage pathway, the final tertiary structure of an S-layer protein bound within the lattice is different to that of the monomeric

form. The rate-limiting factor is the final conformational arrangement in confinement [15, 17]. In addition, the computational approach of studying the reassembly of S-layer proteins *in silico* [41, 44, 132, 133] allows us to gain deeper insight into the (bio)molecular interactions driving the refolding of the proteins, the release of bound water molecules, and the subsequent lattice formation [15, 101, 120].

Finally, we would like to anticipate new challenges when supports with different surface properties are investigated, as described above for the various experimental approaches. Thus, we would like to postulate that S-layer reassembly pathways differ between plain inorganic supports (e.g. gold, silicon dioxide, etc) and SCWP modified surfaces. We assume that the proteins might partially denature on inorganic substrates, while they will assume their correct 3D structure on SCWP-coated surfaces where the correct conformation is stabilized by the specific lectin type binding (figure 6) [83]. This assumption is supported by the observation that larger monocrystalline arrays with higher long-range order are formed on SCWP-coated surfaces compared to plain inorganic ones [92].

In summary, currently there is no other biological matrix known to provide the same outstanding universal properties as self-assembly systems and as patterning elements compared to S-layers. It is tempting to speculate that such a simple protein membrane with the ability for dynamic growth could have fulfilled all necessary barrier functions required by a self-reproducing system during the early stages of biological evolution [115].

Addendum

The terminology 'S-layer' (surface layer) was introduced in 1976 [103] and generally accepted at the First International Workshop on Crystalline Bacterial Cell Surface Layers, in Vienna, Austria, in 1984. Subsequently, at the European Molecular Biology Organization Workshop on Crystalline Bacterial Cell Surface Layers, in Vienna in 1987, S-layers were defined as 'Two-dimensional arrays of proteinaceous subunits forming surface layers on prokaryotic cells' [108].

Acknowledgements

Part of this work was funded by AFOSR Agreement Awards Nr. FA9550-09-0342 and FA9550-12-1-0274 (to DP), and FA9550-10-1-0223 (to UBS), and by the Erwin-Schrödinger Society for Nanosciences, Vienna.

References

[1] Albers S V and Meyer B H 2011 The archaeal cell envelope *Nature Rev. Microbiology* **9** 414–26
[2] Arbing M A, Chan S, Shin A, Phan T, Ahn C J, Rohlin L and Gunsalus R P 2012 Structure of the surface layer of the methanogenic archaean *Methanosarcina Acetivorans Proc. Natl. Acad. Sci. USA* **109** 11812–7
[3] Arnold H *et al* 2010 *International Tables for Crystallography* vol A (Chichester, UK: John Wiley & Sons, Ltd)
[4] Avall-Jaaskelainen S and Palva A 2005 Lactobacillus surface layers and their applications *FEMS Microbiol Rev* **29** 511–29
[5] Baneyx F and Matthaei J F 2014 Self-assembled two-dimensional protein arrays in bionanotechnology: from S-layers to designed lattices *Curr. Opinion Biotechnology* **28** 39–45
[6] Baranova E, Fronzes R, Garcia-Pino A, Van Gerven N, Papapostolou D, Péhau-Arnaudet G, Pardon E, Steyaert J, Howorka S and Remaut H 2012 SbsB structure and lattice reconstruction unveil Ca2+ triggered S-layer assembly *Nature* **487** 119–22
[7] Baumeister W and Engelhardt H 1987 *Electron Microscopy of Proteins* ed J R Harris and R W Horne (London: Academic Press, Inc.) pp 109–54
[8] Baumeister W, Wildhaber I and Phipps B M 1989 Principles of organization in eubacterial and archaebacterial surface proteins *Canadian J. microbiology* **35** 215–27
[9] Ben-Jacob E and Garik P 1990 The formation of patterns in non-equilibrium growth *Nature* **343** 523–30
[10] Bergkvist M, Mark S S, Yang X, Angert E R and Batt C A 2004 Bionanofabrication of ordered nanoparticle arrays: effect of particle properties and adsorption conditions *J. Phys. Chem.* B **108** 8241–8
[11] Bobeth M, Blecha A, Blüher A, Mertig M, Korkmaz N, Ostermann K, Rödel G and Pompe W 2011 Formation of tubes during self-assembly of bacterial surface layers *Langmuir* **27** 15102–11
[12] Breitwieser A, Egelseer E M, Moll D, Ilk N, Hotzy C, Bohle B, Ebner C, Sleytr U B and Sára M 2002 A recombinant bacterial cell surface (S-layer)-major birch pollen allergen-fusion protein (rSbsC/Bet v1) maintains the ability to self-assemble into regularly structured monomolecular lattices and the functionality of the allergen *Protein Eng.* **15** 243–9
[13] Breitwieser A, Gruber K and Sleytr U B 1992 Evidence for an S-layer protein pool in the peptidoglycan of *Bacillus stearothermophilus J. Bacteriol.* **174** 8008–15
[14] Chen J H and Seeman N C 1991 Synthesis from DNA of a molecule with the connectivity of a cube *Nature* **350** 631–3
[15] Chung S, Shin S H, Bertozzi C R and De Yoreo J J 2010 Self-catalyzed growth of S layers via an amorphous-to-crystalline transition limited by folding kinetics *Proc. Natl. Acad. Sci. USA* **107** 16536–41
[16] Claus H and König H 2010 *Prokaryotic Cell Wall Compounds—Structure and Biochemistry* ed H König *et al* (Berlin: Springer-Verlag) pp 231–51
[17] Comolli L R, Siegerist C E, Shin S H, Bertozzi C, Regan W, Zettl A and De Yoreo J 2013 Conformational tranzsitions at an S-layer growing boundary resolved by cryo-TEM *Angew. Chem. Int. Edit.* **52** 4829–32
[18] De Yoreo J 2013 Crystal nucleation: more than one pathway *Nat. Mater.* **12** 284–5
[19] Delcea M, Krastev R, Gutberlet T, Pum D, Sleytr U B and Toca-Herrera J L 2008 Thermal stability, mechanical properties and water content of bacterial protein layers recrystallized on polyelectrolyte multilayers *Soft Matter* **4** 1414–21
[20] Delcea M, Krastev R, Gutlebert T, Pum D, Sleytr U B and Toca-Herrera J L 2007 Mapping bacterial surface layers affinity to polyelectrolytes through the building of hybrid macromolecular structures *J. Nanosci. Nanotech.* **7** 4260–6
[21] Diederich A, Sponer C, Pum D, Sleytr U B and Lösche M 1996 Reciprocal influence between the protein and lipid

components of a lipid-protein membrane model *Coll. Surf.* B **6** 335–46
[22] Dobson C M 2003 Protein folding and misfolding *Nature* **426** 884–90
[23] Ebner A *et al* 2006 Atomic-force-microscopy imaging and molecular-recognition-force microscopy of recrystallized heterotetramers comprising an S-layer-streptavidin fusion protein *Chem. Bio. Chem.* **7** 588–91
[24] Egelseer E M, Ilk N, Pum D, Messner P, Schäffer C, Schuster B and Sleytr U B 2010 *Encyclopedia of Industrial Biotechnology: Bioprocess, Bioseparation, and Cell Technology* ed M C Flickinger (Hoboken, N.J.: John Wiley and Sons) pp 4424–48
[25] Eichler J 2013 Extreme sweetness: protein glycosylation in archaea *Nature Reviews. Microbiology* **11** 151–6
[26] Engelhardt H 2007 Are S-layers exoskeletons? The basic function of protein surface layers revisited *J. Struct. Biol.* **160** 115–24
[27] Engelhardt H and Peters J 1998 Structural research on surface layers: a focus on stability, surface layer homology domains, and surface layer cell wall interactions (review) *J. Struct. Biol.* **124** 276–302
[28] Fagan R P, Albesa-Jove D, Qazi O, Svergun D I, Brown K A and Fairweather N F 2009 Structural insights into the molecular organization of the S-layer from clostridium difficile *Mol. Microbiol.* **71** 1308–22
[29] Fagan R P and Fairweather N F 2014 Biogenesis and functions of bacterial S-layers *Nature Rev. Microbiology* **12** 211–22
[30] Fahmy K, Merroun M, Pollmann K, Raff J, Savchuk O, Hennig C and Selenska-Pobell S 2006 Secondary structure and Pd(II) coordination in S-layer proteins from *Bacillus sphaericus* studied by infrared and x-ray absorption spectroscopy *Biophys. J.* **91** 996–1007
[31] Göbel C, Schuster B, Baurecht D, Sleytr U B and Pum D 2010 S-layer templated bioinspired synthesis of silica *Coll. Surf.* B **75** 565–72
[32] Gruber K and Sleytr U B 1988 Localized insertion of new S-layer during growth of *Bacillus stearothermophilus* strains *Arch. Microbiol.* **149** 485–91
[33] Györvary E, Schroedter A, Talapin D V, Weller H, Pum D and Sleytr U B 2004 Formation of nanoparticle arrays on S-layer protein lattices *J. Nanosci. Nanotech.* **4** 115–20
[34] Györvary E, Wetzer B, Sleytr U B, Sinner A, Offenhäuser A and Knoll W 1999 Lateral diffusion of lipids in silane-, dextrane- and S-layer protein-supported mono- and bilayers *Langmuir* **15** 1337–47
[35] Györvary E S, O'Riordan A, Quinn A J, Redmond G, Pum D and Sleytr U B 2003 Biomimetic nanostructure fabrication: nonlithographic lateral patterning and self-assembly of functional bacterial S-layers at silicon supports *Nano Lett.* **3** 315–9
[36] Györvary E S, Stein O, Pum D and Sleytr U B 2003 Self-assembly and recrystallization of bacterial S-layer proteins at silicon supports imaged in real time by atomic force microscopy *J. Microsc.* **212** 300–6
[37] Hall S R, Shenton W, Engelhardt H and Mann S 2001 Site-specific organization of gold nanoparticles by biomolecular templating *Chem. Phys. Phys. Chem.* **3** 184–6
[38] Handrea M, Sahre M, Neubauer A, Sleytr U B and Kautek W 2003 Electrochemistry of nano-scale bacterial surface protein layers on gold *Bioelectrochem.* **61** 1–8
[39] Harris W F and Scriven L E 1970 Function of dislocations in cell walls and membranes *Nature* **228** 827–9
[40] Harris W F and Scriven L E 1971 Intrinsic disclinations as dislocation sources and sinks in surface crystals *J. Appl. Phys.* **42** 3309–12
[41] Haxton T K and Whitelam S 2012 Design rules for the self-assembly of a protein crystal *Soft Matter* **8** 3558–62
[42] Hirn R, Schuster B, Sleytr U B and Bayerl T M 1999 The effect of S-layer protein adsorption and crystallization on the collective motion of a planar lipid bilayer studied by dynamic light scattering *Biophys. J.* **77** 2066–74
[43] Horejs C, Gollner H, Pum H, Sleytr U B, Peterlik H, Jungbauer A and Tscheliessnig R 2011 Atomistic structure of monomolecular surface layer self-assemblies: toward functionalized nanostructures *ACS Nano* **5** 2288–97
[44] Horejs C, Mitra M K, Pum D, Sleytr U B and Muthukumar M 2011 Monte Carlo study of the molecular mechanisms of surface-layer protein self-assembly *J. Chem. Phys.* **134** 125103
[45] Horejs C, Pum D, Sleytr U B and Tscheliessnig R 2008 Structure prediction of an S-layer protein by the mean force method *J. Chem. Phys.* **128** 65106
[46] Hovmöller S, Sjögren A and Wang D N 1988 The structure of crystalline bacterial surface layers *Prog. Biophys. Mol. Biol.* **51** 131–63
[47] Howard L V, Dalton D D and McCoubrey W K 1982 Expansion of the tetragonally arrayed cell wall protein layer during growth of *Bacillus sphaericus J. Bacteriol.* **149** 748–57
[48] Huber C, Ilk N, Rünzler D, Egelseer E M, Weigert S, Sleytr U B and Sára M 2005 The three S-layer-like homology motifs of the S-layer protein SbpA of *Bacillus sphaericus* CCM 2177 are not sufficient for binding to the pyruvylated secondary cell wall polymer *Mol. Microbiol.* **55** 197–205
[49] Ilk N, Egelseer E M and Sleytr U B 2011 S-layer fusion proteins—construction principles and applications *Curr. Opin. Biotechnol.* **22** 824–31
[50] Ilk N, Schumi C T, Bohle B, Egelseer E M and Sleytr U B 2011 Expression of an endotoxin-free S-layer/allergen fusion protein in gram-positive *Bacillus subtilis* 1012 for the potential application as vaccines for immunotherapy of atopic allergy *Microbial Cell Factory* **10** 6
[51] Ilk N, Völlenkle C, Egelseer E M, Breitwieser A, Sleytr U B and Sára M 2002 Molecular characterization of the S-layer gene, sbpA, of *Bacillus sphaericus* CCM 2177 and production of a functional S-layer fusion protein with the ability to recrystallize in a defined orientation while presenting the fused allergen *Appl. Environ. Microbiol.* **68** 3251–60
[52] Jaenicke R, Welsch R, Sára M and Sleytr U B 1985 Stability and self-assembly of the S-layer protein of the cell wall of *Bacillus stearothermophilus Biol. Chem. Hoppe-Seyler* **366** 663–70
[53] Kern J, Wilton R, Zhang R, Binkowski T A, Joachimiak A and Schneewind O 2011 Structure of surface layer homology (SLH) domains from *Bacillus anthracis* surface array protein *J. Biol. Chem.* **286** 26042–9
[54] Küpcü S, Sára M and Sleytr U B 1995 Liposomes coated with crystalline bacterial cell surface protein (S-layers) as immobilization structures for macromolecules *Biochim. Biophys. Acta* **1235** 263–9
[55] Lopez A E, Moreno-Flores S, Pum D, Sleytr U B and Toca-Herrera J L 2010 Surface dependence of protein nanocrystal formation *Small* **6** 396–403
[56] Mader C, Huber C, Moll D, Sleytr U B and Sára M 2004 Interaction of the crystalline bacterial cell surface layer protein SbsB and the secondary cell wall polymer of *Geobacillus stearothermophilus* PV72 assessed by real-time surface plasmon resonance biosensor technology *J. Bacteriol.* **186** 1758–68
[57] Mader C, Küpcü S, Sára M and Sleytr U B 1999 Stabilizing effect of an S-layer on liposomes towards thermal or mechanical stress *Biochim. Biophys. Acta* **1418** 106–16

[58] Mader C, Küpcü S, Sleytr U B and Sára M 2000 S-layer-coated liposomes as a versatile system for entrapping and binding target molecules *Biochim. Biophys. Acta* **1463** 142–50
[59] Mark S S, Bergkvist M, Yang X, Teixeira L M, Bhatnagar P, Angert E R and Batt C A 2006 Bionanofabrication of metallic and semiconductor nanoparticle arrays using S-layer protein lattices with different lateral spacings and geometries *Langmuir* **22** 3763–74
[60] Mertig M, Kirsch R, Pompe W and Engelhardt H 1999 Fabrication of highly oriented nanocluster arrays by biomolecular templating *Eur. Phys. J.* D **D9** 45–8
[61] Messner P, Pum D, Sára M, Stetter K O and Sleytr U B 1986 Ultrastructure of the cell envelope of the archaebacteria *Thermoproteus tenax* and *Thermoproteus neutrophilus* *J. Bacteriol.* **166** 1046–54
[62] Messner P, Pum D and Sleytr U B 1986 Characterization of the ultrastructure and the self-assembly of the surface layer of *Bacillus stearothermophilus* NRS 2004/3a *J. Ultrastruct. Mol. Struct. Res.* **97** 73–88
[63] Messner P, Schaffer C and Kosma P 2013 Bacterial cell-envelope glycoconjugates *Adv. Carbohydrate Chem. Biochem.* **69** 209–72
[64] Moll D, Huber C, Schlegel B, Pum D, Sleytr U B and Sára M 2002 S-layer-streptavidin fusion proteins as template for nanopatterned molecular arrays *Proc. Natl. Acad. Sci. USA* **99** 14646–51
[65] Moreno-Flores S, Kasry A, Butt H J, Vavilala C, Schmittel M, Pum D, Sleytr U B and Toca-Herrera J L 2008 From native to non-native two-dimensional protein lattices through underlying hydrophilic/hydrophobic nanoprotrusions *Angew. Chem. Int. Ed.* **47** 4707–10
[66] Nabarro F R N and Harris W F 1971 Presence and function of disclinations in surface coats of unicellular organisms *Nature* **232** 423
[67] Norville J E, Kelly D F, Knight T F, Belcher A M and Walz T 2007 7 Å projection map of the S-layer protein sbpA obtained with trehalose-embedded monolayer crystals *J. Struct. Biol.* **160** 313–23
[68] Novotny R, Scheberl A, Giry-Laterriere M, Messner P and Schäffer C 2005 Gene cloning, functional expression and secretion of the S-layer protein SgsE from *Geobacillus stearothermophilus* NRS 2004/3a in *lactococcus lactis* *FEMS Microbiol. Lett.* **242** 27–35
[69] Pavkov T, Egelseer E M, Tesarz M, Svergun D I, Sleytr U B and Keller W 2008 The structure and binding behavior of the bacterial cell surface layer protein SbsC *Structure* **16** 1226–37
[70] Pavkov-Keller T, Howorka S and Keller W 2011 The structure of bacterial S-layer proteins *Prog. Molec. Biol. Transl. Sci.* **103** 73–130
[71] Picher M M, Küpcü S, Huang C J, Dostalek J, Pum D, Sleytr U B and Ertl P 2013 Nanobiotechnology advanced antifouling surfaces for the continuous electrochemical monitoring of glucose in whole blood using a lab-on-a-chip *Lab-on-a-chip* **13** 1780–9
[72] Pum D, Messner P and Sleytr U B 1991 Role of the S layer in morphogenesis and cell division of the archaebacterium methanocorpusculum sinense *J. Bacteriol.* **173** 6865–73
[73] Pum D and Sleytr U B 1994 Large-scale reconstruction of crystalline bacterial surface layer proteins at the air-water interface and on lipids *Thin Solid Films* **244** 882–6
[74] Pum D and Sleytr U B 1995 Anisotropic crystal growth of the S-layer of *Bacillus sphaericus* CCM 2177 at the air/water interface *Coll. Surf.* A **102** 99–104
[75] Pum D and Sleytr U B 1995 Monomolecular reassembly of a crystalline bacterial cell surface layer (S-layer) on untreated and modified silicon surfaces *Supramol. Sci.* **2** 193–7
[76] Pum D and Sleytr U B 2009 *Nanobioelectronics—for Electronics, Biology, and Medicine* ed A Offenhäuser and R Rinaldi (New York: Springer) pp 167–80
[77] Pum D, Toca-Herrera J and Sleytr U 2013 S-layer protein self-assembly *Int. J. Mol. Sci.* **14** 2484–501
[78] Pum D, Weinhandl M, Hödl C and Sleytr U B 1993 Large-scale recrystallization of the S-layer of *Bacillus coagulans* E38-66 at the air/water interface and on lipid films *J. Bacteriol.* **175** 2762–6
[79] Queitsch U, Hamann C, Schaffel F, Rellinghaus B, Schultz L, Bluher A and Mertig M 2009 Toward dense biotemplated magnetic nanoparticle arrays: probing the particle-template interaction *J. Phys. Chem.* C **113** 10471–6
[80] Rhinow D, Vonck J, Schranz M, Beyer A, Golzhauser A and Hampp N 2010 Ultrathin conductive carbon nanomembranes as support films for structural analysis of biological specimens *Phys. Chem. Chem. Phys.* **12** 4345–50
[81] Rothbauer M, Küpcü S, Sticker D, Sleytr U B and Ertl P 2013 Exploitation of s-layer anisotropy: pH-dependent nanolayer orientation for cellular micropatterning *ACS Nano* **7** 8020–30
[82] Rothemund P W K 2006 Folding DNA to create nanoscale shapes and patterns *Nature* **440** 297–302
[83] Rünzler D, Huber C, Moll D, Kohler G and Sara M 2004 Biophysical characterization of the entire bacterial surface layer protein SbsB and its two distinct functional domains *J. Bio. Chem.* **279** 5207–15
[84] Sander L M 1986 Fractal growth processes *Nature* **322** 789–93
[85] Sára M, Dekitsch C, Mayer H F, Egelseer E M and Sleytr U B 1998 Influence of the secondary cell wall polymer on the reassembly, recrystallization, and stability properties of the S-layer protein from *Bacillus stearothermophilus* PV72/p2 *J. Bacteriol.* **180** 4146–53
[86] Sára M, Egelseer E M, Dekitsch C and Sleytr U B 1998 Identification of two binding domains, one for peptidoglycan and another for a secondary cell wall polymer, on the N-terminal part of the S-layer protein SbsB from *Bacillus stearothermophilus* PV72/p2 *J. Bacteriol.* **180** 6780–3
[87] Sára M, Pum D, Küpcü S, Messner P and Sleytr U B 1994 Isolation of two physiologically induced variant strains of *Bacillus stearothermophilus* NRS 2004/3a and characterization of their S-layer lattices *J. Bacteriol.* **176** 848–60
[88] Sára M, Pum D and Sleytr U B 1992 Permeability and charge-dependent adsorption properties of the S-layer lattice from *Bacillus coagulans* E38-66 *J. Bacteriol.* **174** 3487–93
[89] Sára M and Sleytr U B 1987 Molecular sieving through S-layers of *Bacillus stearothermophilus* strains *J. Bacteriol.* **169** 4092–8
[90] Sára M and Sleytr U B 1987 Production and characteristics of ultrafiltration membranes with uniform pores from two-dimensional arrays of proteins *J. Membr. Sci.* **33** 27–49
[91] Sára M and Sleytr U B 2000 S-layer proteins *J. Bacteriol.* **182** 859–68
[92] Schuster B, Pum D and Sleytr U B 2008 S-layer stabilized lipid membranes *Biointerphases* **3** FA3–A11
[93] Schuster B and Sleytr U B 2000 S-layer-supported lipid membranes *Rev. Mol. Biotechnol.* **74** 233–54
[94] Schuster B and Sleytr U B 2005 *Advances in Planar Lipid Bilayers and Liposomes* ed T H Tien and A Ottova (Amsterdam, The Netherlands: Elsevier Science) pp 247–93
[95] Schuster B and Sleytr U B 2009 Composite S-layer lipid structures *J. Struct. Biol.* **168** 207–16
[96] Schuster B and Sleytr U B 2013 *Protein Nanotechnology: Protocols, Instrumentation and Applications* 2nd edn ed J A Gerrard (New York: Humana Press, Springer Science + Business Media) pp 153–75

[97] Schuster D, Küpcü S, Belton D J, Perry C C, Stöger-Pollach M, Sleytr U B and Pum D 2013 Construction of silica enhanced S-layer protein cages *Acta Biomaterialia* **9** 5689–97
[98] Seeman N C 2003 DNA in a material world *Nature* **421** 427–31
[99] Shenton W, Pum D, Sleytr U B and Mann S 1997 Biocrystal templating of CdS superlattices using self-assembled bacterial S-layers *Nature* **389** 585–7
[100] Shin S H, Comolli L R, Tscheliessnig R, Wang C, Nam K T, Hexemer A, Siegerist C E, De Yoreo J J and Bertozzi C R 2013 Self-assembly of 'S-bilayers', a step toward expanding the dimensionality of S-layer assemblies *ACS Nano* **7** 4946–53
[101] Shin S H, Chung S, Sanii B, Comolli L R, Bertozzi C R and De Yoreo J J 2012 Direct observation of kinetic traps associated with structural transformations leading to multiple pathways of S-layer assembly *Proc. Natl. Acad. Sci. USA* **109** 12968–73
[102] Sleytr U B 1975 Heterologous reattachment of regular arrays of glycoproteins on bacterial surfaces *Nature* **257** 400–2
[103] Sleytr U B 1976 Self-assembly of the hexagonally and tetragonally arranged subunits of bacterial surface layers and their reattachment to cell walls *J. Ultrastruct. Res.* **55** 360–77
[104] Sleytr U B 1978 Regular arrays of macromolecules on bacterial cell walls: structure, chemistry, assembly, and function *Int. Rev. Cytol.* **53** 1–64
[105] Sleytr U B, Egelseer E M, Ilk N, Pum D and Schuster B 2007 S-layers as a basic building block in a molecular construction kit *FEBS Journal* **274** 323–34
[106] Sleytr U B, Huber C, Ilk N, Pum D, Schuster B and Egelseer E M 2007 S-layers as a tool kit for nanobiotechnological applications *FEMS Microbiol. Lett.* **267** 131–44
[107] Sleytr U B and Messner P 1989 *Electron Microsc. of Subcellular Dynamics* ed H Plattner (Boca Raton, FL: CRC Press) pp 13–31
[108] Sleytr U B, Messner P, Pum D and Sára M eds1988 *Crystalline Bacterial Cell Surface Layers* (Berlin: Springer)
[109] Sleytr U B, Messner P, Pum D and Sára M 1999 Crystalline bacterial cell surface layers (S layers): from supramolecular cell structure to biomimetics and nanotechnology (review) *Angew. Chem. Int. Ed.* **38** 1035–54
[110] Sleytr U B and Plohberger R 1980 *Electron Microsc. at Molecular Dimensions* ed W Baumeister and W Vogell (Berlin: Springer-Verlag) pp 36–47
[111] Sleytr U B, Pum D, Egelseer E M, Ilk N and Schuster B 2013 *Handbook of Biofunctional Surfaces* ed W Knoll (Singapore: Pan Stanford Publishing) pp 507–68
[112] Sleytr U B, Sára M and Kautek W 2004 Method for producing a layer of functional molecules *US Patent Number* 20040137527A1
[113] Sleytr U B, Sara M, Mader C, Schuster B and Unger F M 2006 Use of secondary cell wall polymer of procaryotic microorganisms *US Patent Number* 7,125,707 B2
[114] Sleytr U B, Sára M, Pum D and Schuster B 2005 *Supramolecular Polymers* ed A Ciferri (Boca Raton, FL: Taylor and Francis) pp 583–616
[115] Sleytr U B, Schuster B, Egelseer E M and Pum D 2014 S-layers: principles and applications *FEMS Microbiol Rev.* at press
[116] Sleytr U B, Schuster B, Egelseer E M, Pum D, Horejs C M, Tscheliessnig R and Ilk N 2011 Nanobiotechnology with S-layer proteins as building blocks *Prog. Molec. Biol. Translat. Sci.* **103** 277–352
[117] Smit J and Todd W J 1986 *Ultrastructure Techniques for Microorganisms* ed H C Aldrich and W J Todd (New York: Plenum Press) pp 469–519
[118] Sotiropoulou S, Mark S S, Angert E R and Batt C A 2007 Nanoporous S-layer protein lattices. a biological ion gate with calcium selectivity *J. Phys. Chem.* C **111** 13232–7
[119] Tang J, Ebner A, Huber C, Ilk N, Zhu R, Pastushenko V, Sára M and Hinterdorfer P 2007 High resolution atomic force microscopy imaging and single molecule force microscopy studies of S-layer-strep-tag I and S-layer-strep-tag II proteins *Biophys. J. (**Suppl. S**)* 513A
[120] Teixeira L M, Strickland A, Mark S S, Bergkvist M, Sierra-Sastre Y and Batt C A 2010 Entropically driven self-assembly of *Lysinibacillus sphaericus* S-layer proteins analyzed under various environmental conditions *Macromol Biosci* **10** 147–55
[121] tenWolde P R and Frenkel D 1997 Enhancement of protein crystal nucleation by critical density fluctuations *Science* **277** 1975–8
[122] Toca-Herrera J L, Krastev R, Bosio V, Küpcü S, Pum D, Fery A, Sára M and Sleytr U B 2005 Recrystallization of bacterial S-layers on flat polyelectrolyte surfaces and hollow polyelectrolyte capsules *Small* **1** 339–48
[123] Ücisik M H, Küpcü S, Debreczeny M, Schuster B and Sleytr U B 2013 S-layer coated emulsomes as potential nanocarriers *Small* **9** 2895–904
[124] Ulman A 1991 *An Introduction to Ultrathin Organic Films* (Boston: Academic Press)
[125] Ulman A 1996 Formation and structure of self-assembled monolayers *Chem Rev* **96** 1533–54
[126] Vyalikh D V, Danzenbächer S, Mertig M, Kirchner A, Pompe W, Dedkov Y S and Molodtsov S L 2004 Electronic structure of regular bacterial surface layers *Phys. Rev. Lett.* **93** 238103-1-4
[127] Wetzer B, Pfandler A, Györvary E, Pum D, Lösche M and Sleytr U B 1998 S-layer reconstitution at phospholipid monolayers *Langmuir* **14** 6899–906
[128] Wetzer B, Pum D and Sleytr U B 1997 S-layer stabilized solid supported lipid bilayers *J. Struct. Biol.* **119** 123–8
[129] Weygand M, Kjaer K, Howes P B, Wetzer B, Pum D, Sleytr U B and Lösche M 2002 Structural reorganization of phospholipid headgroups upon recrystallization of an S-layer lattice *J. Phys. Chem.* B **106** 5793–9
[130] Weygand M, Schalke M, Howes P B, Kjaer K, Friedmann J, Wetzer B, Pum D, Sleytr U B and Lösche M 2000 Coupling of protein sheet crystals (S-layers) to phospholipid monolayers *J. Mat. Chem.* **10** 141–8
[131] Weygand M, Wetzer B, Pum D, Sleytr U B, Cuvillier N, Kjaer K, Howes P B and Losche M 1999 Bacterial S-layer protein coupling to lipids: x-ray reflectivity and grazing incidence diffraction studies *Biophys. J.* **76** 458–68
[132] Whitelam S 2010 Control of pathways and yields of protein crystallization through the interplay of nonspecific and specific attractions *Phys. Rev. Lett.* **105** 088102
[133] Whitelam S 2010 Nonclassical assembly pathways of anisotropic particles *J. Chem. Phys.* **132** 194901
[134] Whitesides G M, Mathias J P and Seto C T 1991 Molecular self-assembly and nanochemistry—a chemical strategy for the synthesis of nanostructures *Science* **254** 1312–9
[135] Wildhaber I and Baumeister W 1987 The cell envelope of *thermoproteus tenax*: three-dimensional structure of the surface layer and its role in shape-maintainance *EMBO J.* **6** 1475–80
[136] Winfree E, Liu F, Wenzler L A and Seeman N C 1998 Design and self-assembly of two-dimensional DNA crystals *Nature* **394** 539–44
[137] De Yoreo J J, Chung S and Nielsen M H 2013 The dynamics and energetics of matrix assembly and mineralization *Calcif. Tissue Int.* **93** 316–28